ACS APPLIED MATERIALS & INTERFACES

RESEARCH ARTICLE

www.acsami.org

Double-Layer Imprint Lithography on Wafers and Foils from the Submicrometer to the Millimeter Scale

Pieter F. Moonen,[†] Iryna Yakimets,[‡] Mariá Péter,[‡] Erwin R. Meinders,[‡] and Jurriaan Huskens[†,*]

[†]Molecular Nanofabrication Group, MESA+ Institute for Nanotechnology, University of Twente, P.O. Box 217, 7500 AE Enschede, The Netherlands

[‡]Holst Centre/TNO, High Tech Campus 31, 5656 AE Eindhoven, The Netherlands

Supporting Information

ABSTRACT: In this paper, a thermal imprint technique, double-layer nanoimprint lithography (dlNIL), is introduced, allowing complete filling of features in the dimensional range of submicrometer to millimeter. The imprinting and filling quality of dlNIL was studied on Si substrates as a model system and compared to results obtained with regular NIL (NIL) and reverse NIL (rNIL). Wavy foils were imprinted with NIL, rNIL and dlNIL and the patterning results compared and discussed. With dlNIL, a new application possibility was introduced in which two different resists having, for example, a different etch resistance to a certain plasma were combined within one imprint step. dlNIL allows extension to many resist combinations for tailored nanostructure fabrication.

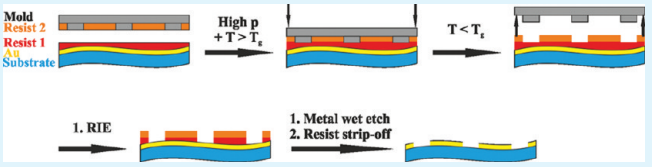

KEYWORDS: thermal nanoimprint lithography, multidimensional pattern transfer, heterogeneous polymer bonding, flexible substrates

INTRODUCTION

The fabrication of micro- to nanoscale structures of a wide variety of rigid and flexible materials is of large interest for the semiconductor industry and for nanoscience in general. Nanoimprint lithography (NIL),[1,2] first discovered by Chou et al.[3,4] is seen as one of the next generation lithography techniques addressing the need for low-cost, high-resolution and high-throughput manufacturing of high-density integrated circuits and optics. In addition to the fabrication of rigid microchips, NIL can also be used as structuring technique in the fabrication of flexible electronic devices and it is suitable for large-area production in both sheet-to-sheet and roll-to-roll (e.g., Roller NIL[5]) configurations. The enhanced functionality (bendable, rollable) combined with the low-weight and possible transparency of flexible devices enables high-level integration into products and systems such as mobile phones, E-readers and thin-film-transistor (TFT) displays. However, surface flatness and the dimensional stability of the flexible substrates need to be controlled to obtain good registration accuracy for multilayer devices, such as thin-film transistors.

A lot of NIL processes were developed over the past 15 years, concerning different types of substrates, resist materials and molding processes. Continuous imprinting techniques, such as step-and-repeat imprint lithography (step-and-stamp IL[6,7] for thermal resists, step-and-flash IL[8,9] for UV resists) and roll-to-roll NIL[10] have been invented for an increased throughput. Nonflat surfaces can be patterned with rigiflex molds[11] or reverse NIL (rNIL).[12,13] Small and large features can be patterned by hybrid solutions combining NIL and conventional photolithography (combined nanoimprint- and photolithography; CNP.[14]

In imprint lithography, mold filling and polymer release are important factors to successful thermal embossing. Numerous studies have been carried out by a broad range of researchers,[15−22] discovering a strong dependence of polymer squeeze and shear flow as function of the cavity geometry, polymer film thickness and viscoelastic properties from the 10-nm to the 1-mm scale. Depending on the architecture of the desired structure (aspect ratio, duty cycle) inhomogeneous single peak or dual peak deformation of the polymer occurs. Small cavities fill first, unless the local cavity width is less than the film thickness. In that case constrained single peak flow occurs.[23] The technique of rNIL was developed to overcome filling issues in large features, experienced with regular NIL. In rNIL, the resist is applied to the mold rather than the substrate. The resist fills the protrusions of the mold during deposition (e.g., spincoating) and is transferred to the substrate during imprinting. Arbitrarily sized features can be imprinted without filling issues. Simultaneous filling of small and large features over a wide dimensional range has not been reported for rNIL.

In this report, the resist filling behavior and simultaneous pattern transfer of features over a wide dimensional range, from the submicrometer to the mm regime, on rigid and flexible substrates such as commercially available thin plastic foils, are studied. Double layer NIL (dlNIL), a technique based on polymer bonding lithography developed by Borzenko et al.,[24] is used to combine homogeneous and heterogeneous resist layers applied to both the mold and the substrate. The mold filling

Received: December 3, 2010
Accepted: February 28, 2011
Published: March 11, 2011

dx.doi.org/10.1021/am101187n | ACS Appl. Mater. Interfaces 2011, 3, 1041–1048

Scheme 1. Process Flows of NIL, rNIL, and dlNIL Leading to Direct Etching of (A) an Underlying Metal Layer or (B) a Metal Pattern after Evaporation and Lift-off[a]

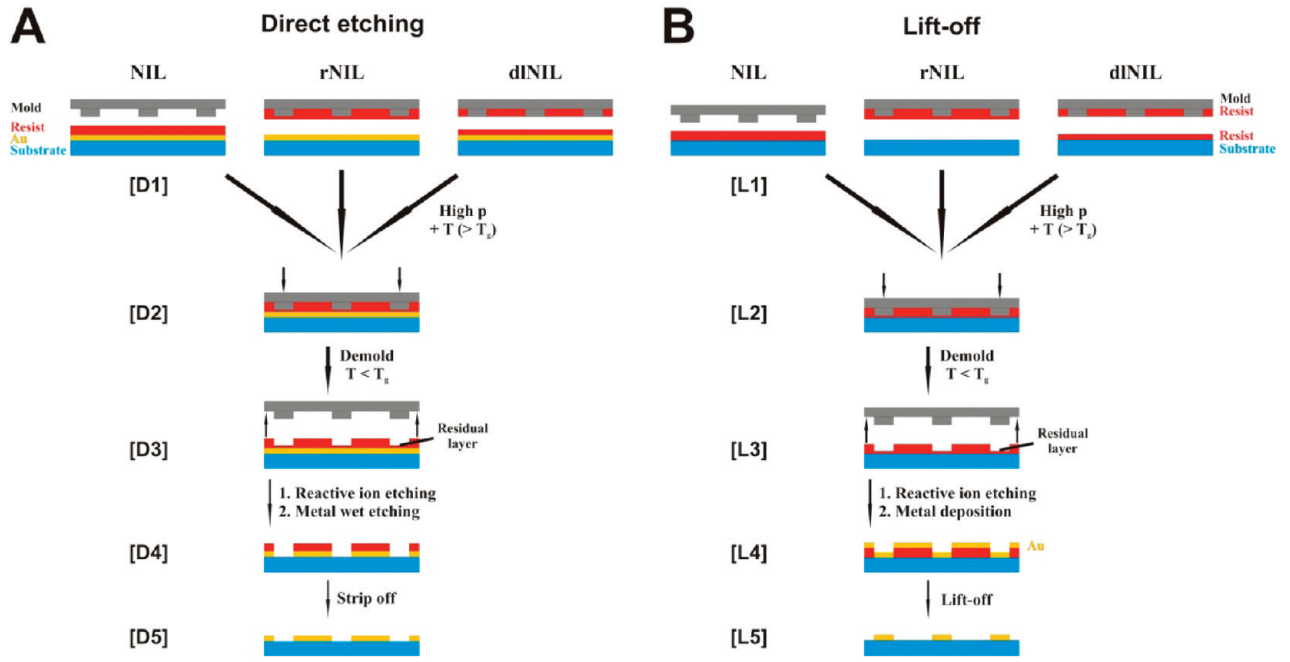

[a] [D1]/[L1]: Resist is deposited on the substrate (NIL), the template (rNIL), or on both (dlNIL). [D2]/[L2]: Under the influence of pressure and temperature the resist is imprinted, followed by a demolding step below T_g. [D3]/[L3]: The residual layer is removed by anisotropic RIE opening windows in the resist layer. The inverse patterns are obtained by [D4] wet etching and subsequent [D5] resist strip-off. Patterns are obtained by [L4] metal deposition and [L5] subsequent lift-off.

quality and pattern transfer results on Si wafers are compared to imprint results obtained with the existing thermal imprint techniques regular NIL and rNIL. Pattern transfer results obtained by imprinting on nonflat surfaces (foils glued to a carrier) with NIL, rNIL and dlNIL are also compared and discussed. An interesting new possibility of the dlNIL technique is given: a patterned two-layer resist on rigid and on nonflat surfaces using different resists as top and bottom layer, thereby smartly making use of different etch rates or surfaces energies of the two resists for example.

RESULTS AND DISCUSSION

Design and Process Scheme. Scheme 1 shows the process flows of the imprint lithography techniques discussed here, NIL, rNIL and dlNIL, displayed both in a direct metal etch ([D1-D5]) and lift-off ([L1-L5]) fashion. Depending on the imprint technique, the thermoplastic resist is deposited by spincoating on the substrate (NIL), on the mold (rNIL), or on both the substrate and the mold (dlNIL).

Si wafers and 125 μm thick poly(ethylene naphthalate) (PEN) foils reversibly glued to a carrier (foil-on-carrier; FOC) were used as substrates. Substrates used in the direct etch approach were covered with a thin metal layer before resist deposition.

An antisticking layer, typically 1H,1H,2H,2H-perfluorodecyltrichlorosilane (PFDTS) or octadecyltrichlorosilane (OTS) (see below) deposited on the mold, is required to guarantee complete transfer of the imprinted resist to the substrate during demolding. The mold contains line and square features in the dimensional range of 1.0 μm up to 1.4 mm with a depth of 200 nm. The mold is pressed for a time t_{imp} into the resist at a temperature T_{imp} well above the glass transition temperature (T_g) of the thermoplastic resist ([D2] and [L2]). MrI7020E was chosen being a dedicated imprint resist with a T_g (60 °C) well below the T_g of PEN (120 °C). Above T_g, the viscosity of the resist lowers allowing the mold protrusions to be filled. After cooling down below T_g demolding can occur, separating the template from the resist ([D3] and [L3]). A thin residual layer remains on the imprinted substrate, which is removed by anisotropic reactive ion etching (RIE) using O_2 plasma opening windows in the resist layer. In the direct etching process (Scheme 1A), the uncovered metal layer (30 nm gold +5 nm Ti adhesion layer) is removed by wet etching ([D4]) and the process is finished by stripping off the resist in O_2 plasma or an adequate solvent ([D5]). When following the lift-off route (Scheme 1B), metal is deposited after residual layer removal ([L4]). The lift-off process is finished by dissolving the resist, simultaneously removing all metal deposited on top of it ([L5]). With direct etching an inverted pattern and with lift-off a replica of the original mold pattern is obtained.

Regular NIL. Regular NIL was applied on a Si wafer using an OTS-coated mold and mrI7020E (T_g= 60 °C) as the resist, at a pressure of 40 bar for 300 s at 140 °C. Demolding occurred at 55 °C.

The optical microscopy images in Figure 1 show regular NIL-patterned resist on Si. Features of 200 μm square pads connected to 5 μm wide and spaced lines were well replicated, showing a reasonably homogeneous residual layer and filling deduced from the absence of color deviations. The narrow 1.0 μm-spaced 10 μm-wide lines (b) and the large 1.4 mm square pad (c) are replicated, both showing inhomogeneous filling effects (color deviations) and a secondary structure on top of the resist (See Figure S4a for a SEM cross section image of the edge of a NIL patterned 200 μm wide pad).

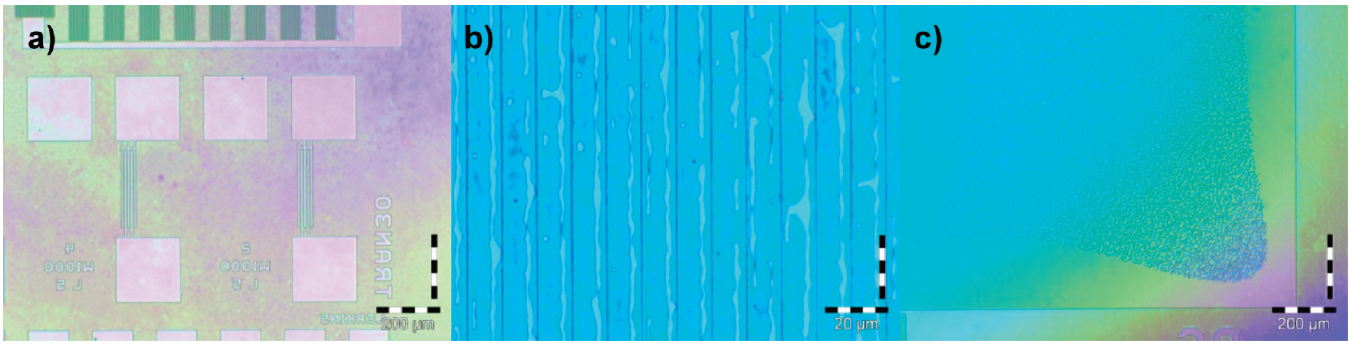

Figure 1. Optical microscopy images of thermal NIL-patterned mrI7020E resist on Si with an OTS-coated template. (a) Interdigitated 5 μm spaced source-drain fingers connected to 200 μm contact pads. Dewetting patterns are visible on top of (b) the narrowest 1 μm spaced lines and (c) the largest 1.4 mm wide imprinted features.

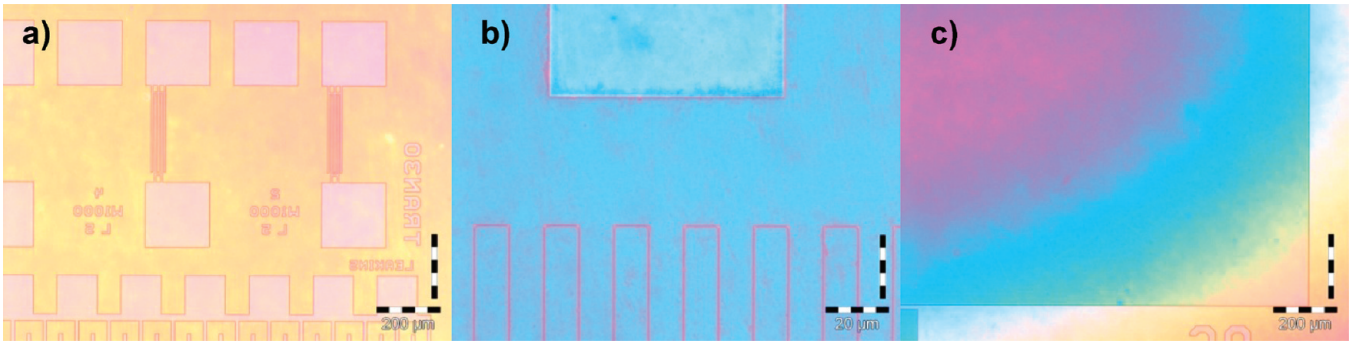

Figure 2. Optical microscopy images of rNIL-patterned mrI7020E resist on Si with an OTS-coated template. All features over the entire 4 in. wafer were transferred and filled entirely. (a) Five-micrometer-wide interdigitated fingers connected to 200 μm contact pads. No dewetting patterns were observed in (b) the narrowest 1.0 μm spaced 10 μm wide lines and (c) the largest 1.4 mm features.

An improved filling might be obtained by raising the temperature and pressure even further, to improve the fluido-dynamic behavior of the high viscosity polymer. On the other hand, higher temperatures and pressures are undesirable characteristics in device fabrication, and alternative processes are more promising.[24]

The additional structures visible on the narrow spaced lines and on the large (>200 μm) features are attributed to the resist dewetting from the OTS antisticking layer of the mold (contact angle of 98.2° ± 0.3[25]) during imprinting. Some structure resulting from this dewetting apparently remains on top of the imprinted features after demolding. Imprinting results obtained with a PFDTS antisticking layer, which has a lower surface energy (static water contact angle 109.6° ± 0.4[25]), showed a stronger dewetting effect (see Supporting Information). OTS and PFDTS showed both good antisticking layer properties, as all resist was in all experiments completely transferred to the substrate. No resist remained on the mold.

With regular NIL, (small) features in the dimensional range of 1.0 μm − ~150 μm could be transferred with good reproducibility over the whole 4" Si wafer. Larger features (>200 μm) however, and unpatterned open areas were often incompletely filled as visualized by the color deviations in the optical microscope images in Figure 1.

Reverse NIL. In reverse NIL (rNIL),[12] the thermoplastic resist is spincoated on the template (Scheme 1). The advantage of this procedure is the direct filling of the cavities before imprinting, promising complete filling without suffering from a thinner resist layer in the center of large features.

rNIL was applied on a Si wafer using an OTS-coated mold and mrI7020E as resist, under 40 bar pressure for 300 s at 140 °C. Demolding occurred at 55 °C.

Figure 2 shows optical microscope images of rNIL-patterned resist on Si (See Figure S4b for a SEM cross section image of the edge of a rNIL patterned 200 μm wide pad). Features of 200 μm up to 1.4 mm (c) were entirely filled, not suffering from the incomplete filling observed during regular NIL. Also dewetting was no longer observed on the 1.0 μm-spaced, 10 μm-wide lines and on the largest 1.4 mm feature (Figure 2b,c). Except for the largest features (Figure 2c), the residual layer thickness and imprint height appeared to be fairly homogeneous, as deduced from the absence of color deviations (Figure 2a,b).

All features on the mold, from 1.0 μm to 1.4 mm, could be replicated with rNIL by use of an OTS antisticking layer, allowing completely and homogeneously filled mold protrusions. Initial imprints with PFDTS as antisticking layer, resulted only in partial transfer of small and large features with and without residual layer (see Supporting Information). An observed problem with rNIL is lack of resist transfer from not fully filled mold protrusions. If the resist does not contact the substrate during imprinting, it is not transferred and remains in the mold cavities.

Double-Layer NIL. In double layer NIL (dlNIL), a technique based on polymer bonding lithography,[24] a thin thermoplastic resist layer is spincoated on the substrate and on the mold. Above T_g both resist layers merge. This constitutes a major advantage of dlNIL, as it allows the combination of two different resists (see below). With dlNIL, the resist present on the substrate flows into

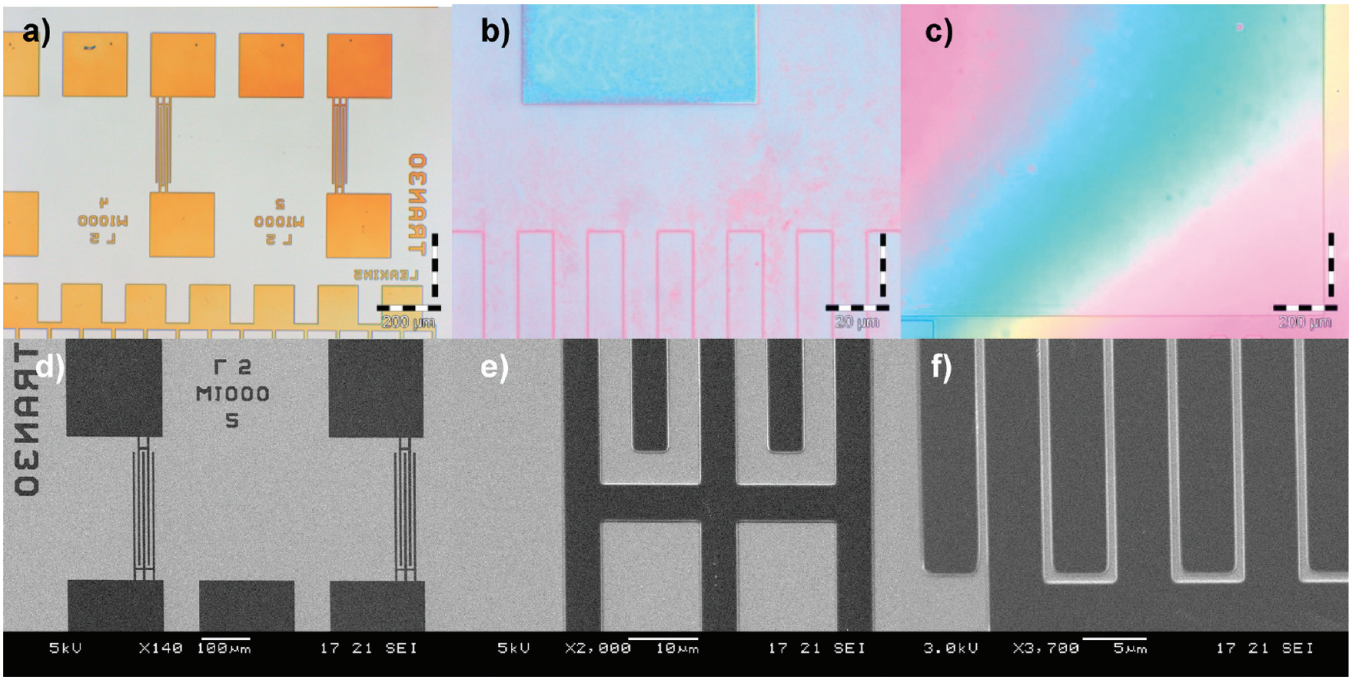

Figure 3. Optical microscopy and SEM images of dlNIL-patterned thermoplastic resist on Si with an OTS-coated mold directly after imprinting. Resist mrI7000E in a 100 nm and a 200 nm layer thickness was applied on the mold respectively the substrate. All features over the entire 4 in. wafer were transferred and filled completely without obvious dewetting patterns. (a, d, e) 5 μm-wide interdigitated fingers connected to 200 μm contact pads. No dewetting patterns could be observed in (b) the narrowest 750 nm-spaced lines and (c) the largest 1.4 mm features. (f) SEM image of 1.4 μm spaced lines.

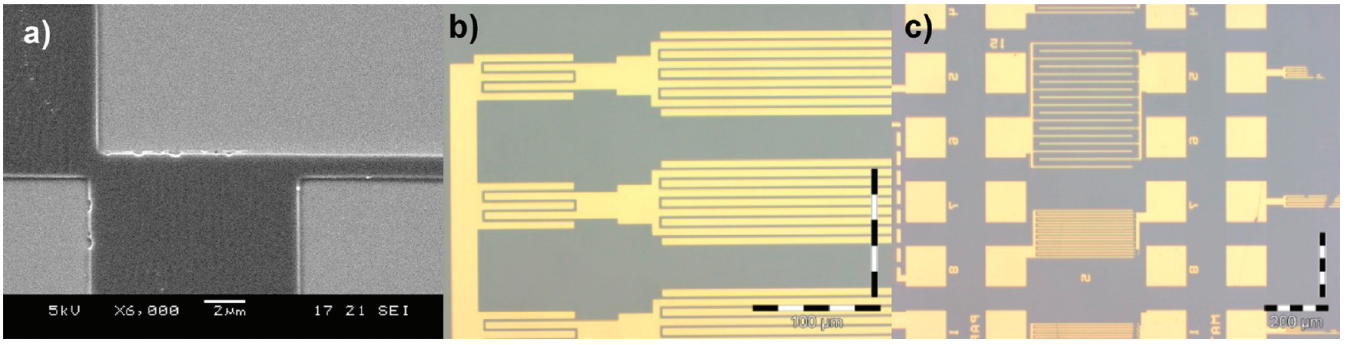

Figure 4. dlNIL-patterned features with an OTS-coated mold on Si after residual layer removal with RIE, Au and Ti wet etching and resist strip-off. (a) SEM image of the smallest patterned line feature with a width of 1 μm. Optical microscope images of (b) 5 μm wide interdigitated 2.5 μm spaced lines and (c) 4 μm wide, 5 and 20 μm spaced lines connected to 125 μm contact pads.

the not fully filled protrusions of the mold and combines with the resist spincoated on the mold. During demolding below T_g, the entire imprinted resist layer is transferred to the substrate, leaving no residues in the mold protrusions (Scheme 1).

For dlNIL, the resist was spin-coated on the substrate and on the OTS-coated mold, and was imprinted at 140 °C under 40 bar pressure for 300 s. Optical microscope and SEM images (Figure 3) show a range of features patterned by dlNIL on Si. For SEM imaging, 5 nm Au/Pd 80%/20% was deposited on top of the imprinted features. The 200 μm pads (a) and larger features of 1.4 mm (c) were entirely transferred, not suffering from opened windows in the middle of the features due to lack of filling during imprinting (see Figure S4c for a SEM cross section image of the edge of a dlNIL patterned 200 μm wide pad). Dewetting was no longer observed for the 1.0 μm-spaced lines (b) and the largest 1.4 mm features (c), similar to rNIL. Except for the largest feature (c), the residual layer thickness and imprint height appeared to be homogeneous. The SEM pictures (d-f) show the high quality of dlNIL-patterned interdigitated 5 μm-wide and spaced lines (d, f) and a 1.4 μm-spaced line structure (f).

Figure 4 shows gold features visible on Si, made by dlNIL and subsequent wet etching and resist strip-off (Scheme 1A). The smallest patterned feature is a 4-point-probe architecture of a 1.0 μm-wide line connected to 125 μm-sized contact pads (a). Interdigitated lines of 5 μm width spaced by 2.5 μm in (b) and 4 μm wide lines spaced by 5 and 20 μm connected to 125 μm contact pads show the quality of dlNIL-patterned metal structures.

Thermal imprinting was not only performed on Si wafers, but also on 125 μm thick PEN foil reversibly glued to a carrier

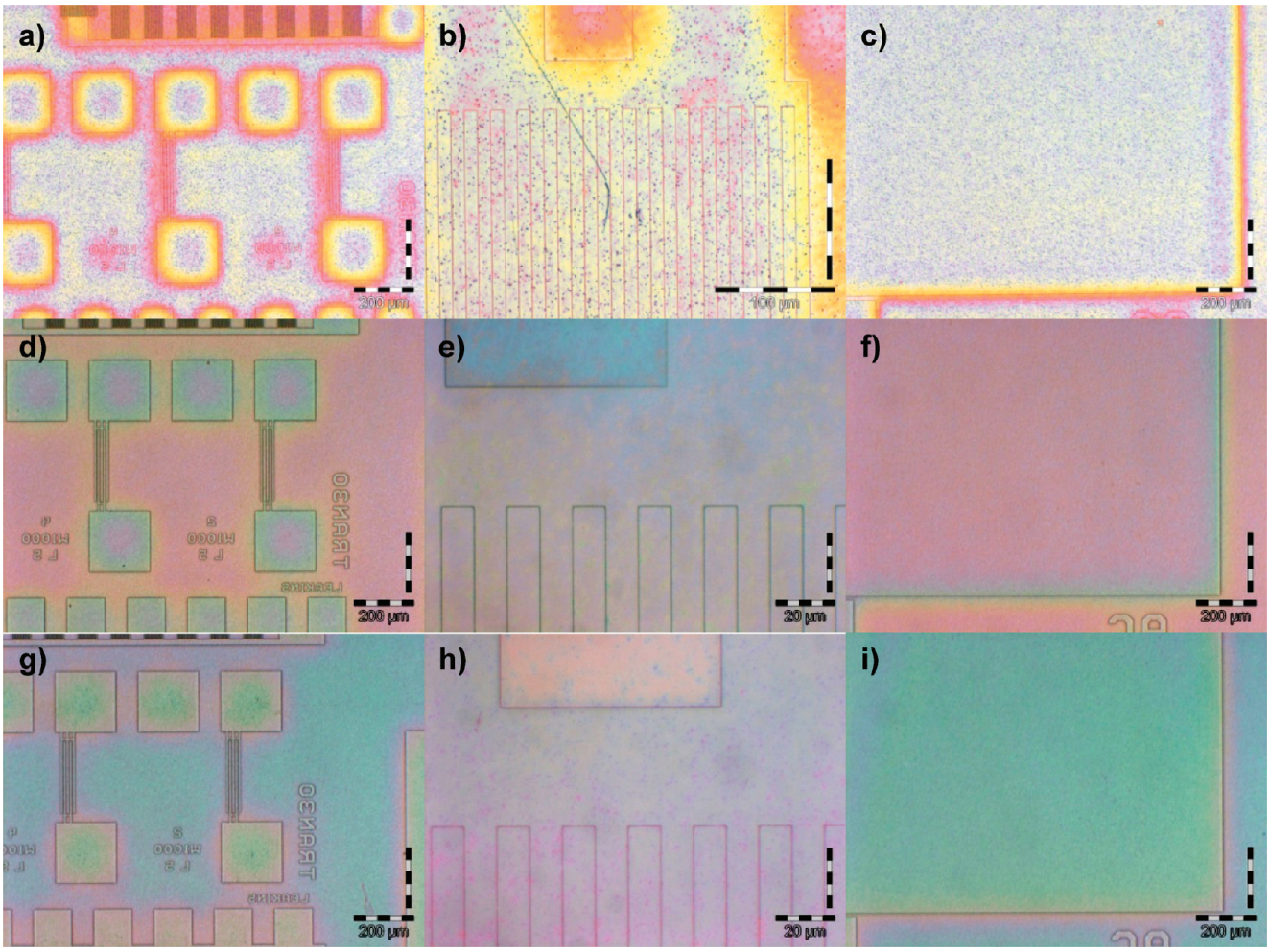

Figure 5. Optical microscopy images of (a−c) NIL, (d−f) rNIL, and (g−i) dlNIL-patterned thermoplastic resist on FOC with an OTS-coated template. In (a, d, g) 5 μm-wide and spaced interdigitated fingers connected to 200 μm-wide contact pads, in (b, e, h) 1 μm-spaced lines and in (c, f, i) a part of the largest 1.4 mm wide feature are shown.

(foil-on-carrier, FOC). With NIL, rNIL and dlNIL these FOCs were patterned under the same conditions as their Si wafer counterparts using an OTS-coated Si mold at 140 °C under 40 bar pressure.

The flexibility and waviness of foils makes faithful pattern replication more difficult when compared to imprinting on Si substrates. With the FOC approach, the flexibility and waviness were drastically reduced to an overall waviness of 1.5 μm within the substrate. The difficulty lies in the inhomogeneous filling of resist in the hills and valleys of the foil, resulting in an inhomogeneous overall residual layer thickness. During RIE, the breakthrough of the residual layer occurs earlier on the hills (thinner residual layer) than in the valleys. Residual layer removal in the valleys therefore may occur concurrently with imprint pattern removal on the hills. The etching problem occurring for varying residual layer thicknesses is tackled by the combination of two different resists, as is discussed below.

Figure 5 shows optical microscope images of resist patterned by NIL, rNIL and dlNIL on FOC. Cross sectional images by lamella cutting with focused ion beam (FIB) were unsuccessful due to the low T_g (60 °C) of the imprint resist. The same sets of features are compared for all three techniques. Similar to the results obtained for patterning on Si with regular NIL, the larger (>150 μm) features could not be filled completely on FOC. Strong height differences in the resist layer thickness from the edge to the center of the feature are indicated by the color deviations in the optical microscopy images. Also here, this is attributed to two-peak filling behavior.

Imprinting with the rNIL and dlNIL techniques resulted in homogeneous resist and residual layer thicknesses and in pattern transfer of the entire imprinted range of 1.0 μm up to 1.4 mm features to the FOC with no major difference with respect to the filling quality. With NIL, inhomogeneous filling of the larger features, visible in the contact pads in Figure 5a, and the lowest patterning quality were observed.

With dlNIL it is not only possible to pattern with high quality over a large dimensional range of features on Si and foil, but it also allows the combination of two resists with different properties. A potential application is shown in Scheme 2. A resist (resist 2), with for example a high oxygen plasma resistivity, is deposited on the mold, while a more oxygen sensitive resist (resist 1) is deposited on the substrate. Resist 1, deposited on the wavy foil, acts as pattern transfer layer for not completely and homogeneously with resist 2 filled protrusions on the mold, and ensures additionally a conformal contact between substrate and resist 2. An inhomogeneous resist layer thickness is often observed with wavy substrates

Scheme 2. Process Flow of dlNIL with the Higher Etch Resistant Resist 2 Deposited on the Mold and Resist 1 Deposited on the Substrate[a]

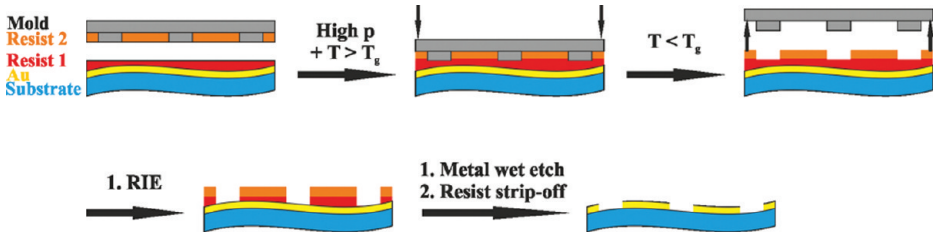

[a] At a temperature of $T > T_g$, the mold is pressed onto resist 1. Demolding at a temperature below T_g transfers resist 2 to 1. RIE is used to remove the thin residual layer, if at all present. Resist 1 is etched with resist 2 serving as etch mask. With a good etch selectivity the waviness of the substrate is compensated and RIE opens windows in resist 1 to the metal. The metal can be removed by wet etching. Resist is stripped-off by plasma treatment or solvent.

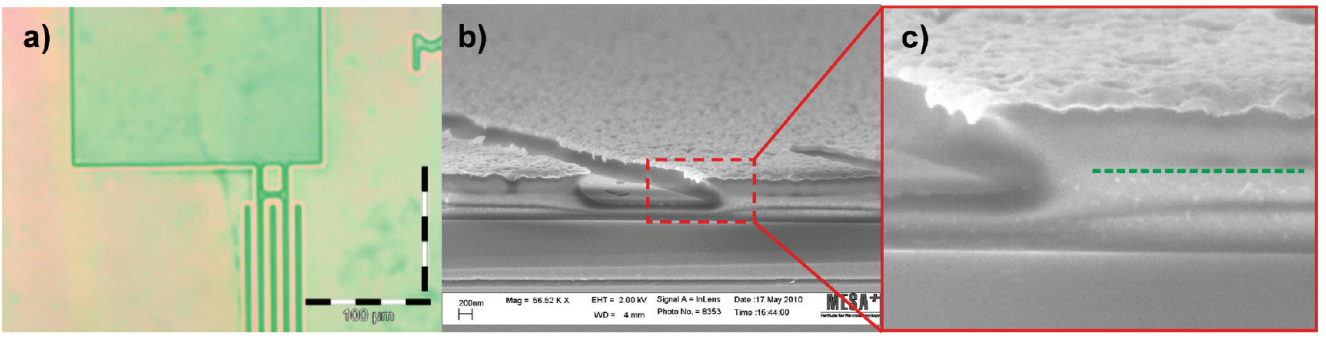

Figure 6. dlNIL-patterned mrI-T85 resist transferred to a PMMA bottom layer deposited on the substrate. (a) Optical microscope image displaying 5 μm wide and spaced interdigitated fingers connected to a 200 μm contact pad. (b, c) SEM images showing the imprinted mrI-T85 resist on top of the PMMA bottom layer on Si with the interface indicated by the green dashed line in (c).

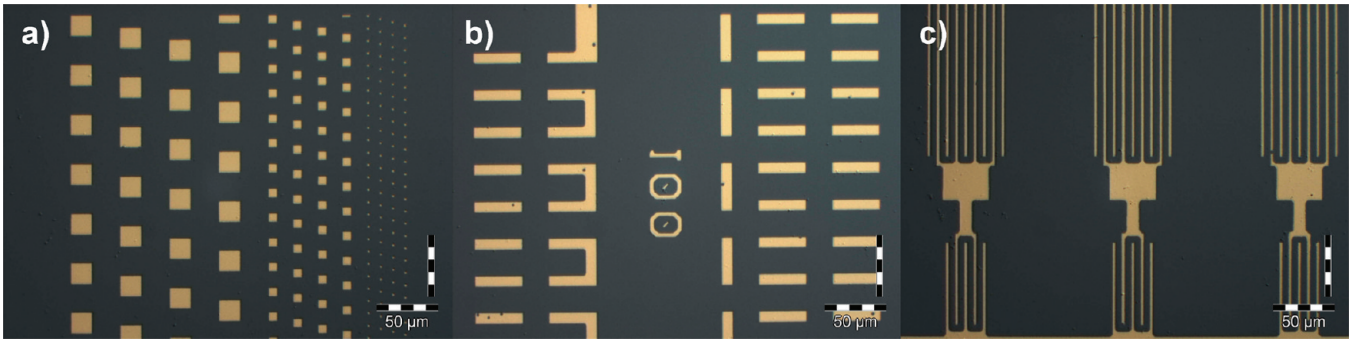

Figure 7. Optical microscopy images of dlNIL-patterned features with an OTS-coated mold on Si after RIE of the residual layer and unprotected PMMA, Au, and Ti wet etching and resist strip-off: (a) 1.5, 7, and 17 μm wide squares; (b) 40 μm long, 4 μm wide rectangles; and (c) 1.5 μm wide, 5 μm spaced lines connected to a 40 μm pad.

(foil), as hills and valleys are differentially filled. The here shown, heterogeneous combination of two resists with dlNIL allows removal of the entire residual layer, benefitting from the higher etch resistivity of the top imprinted resist toward oxygen RIE, compensating the thinner residual layers on top of the hills of the wavy foil. Resist 2 can be etched, for example with fluorine-based plasma, until it breaks through to resist 1, after which O_2 RIE is used to etch resist 1 down to the substrate level. With a good etch selectivity between both resists, resist 2 acts as etch mask for resist 1, resulting in inverted features.

To prove the possibility of combining two resists with dlNIL, poly(methylmethacrylate) (PMMA) was spincoated on a Si substrate and resist mrI-T85 on the OTS-coated mold. Figure 6 shows an optical microscope image showing 5 μm wide and spaced lines connected to a 200 μm large pad. The SEM cross section images display the two different resist layers. The green dashed line in Figure 6c (a magnification of Figure 6b) indicates the interface between the PMMA layer and the mr-IT85 resist. The imprinted mrI-T85 resist was successfully transferred from the mold to the PMMA bottom layer.

As outlined in Scheme 2, the unprotected gold can be wet etched after removal of the residual layer of the top resist (resist 2) and the unprotected resist 1 by RIE. As last step in the process, remaining resist is removed by a strip of in O_2 plasma. Metal

structures obtained by the presented dlNIL process with two different resists are shown in Figure 7.

The combination of two resists with dlNIL by applying one to the mold and the other to the substrate is an easy and good working transfer method. The top resist is effectively working as etch mask for the less etch resistant PMMA resist. The here reported technique allows combination of resists not accessible to regular NIL. For instance, undercut structures for lift-off can be fabricated, but also the combination of two heterogeneous resists with different surface energy to control wetting could be thought off.

CONCLUSIONS

Resist layers were patterned by three thermal imprinting techniques, namely regular NIL, rNIL and dlNIL, on Si substrates as a model system with an OTS-coated Si mold. With regular NIL, small (<150 μm) features could be patterned, but larger features were not entirely filled with an inhomogeneous residual layer thickness as result. On the largest 1.4 mm features the resist in the center of the square feature was removed by RIE before the residual layer on other features could be etched away.

The other two techniques, rNIL and dlNIL, both give access to fully patterned and well transferred resist layers on Si and FOC over an area of 100 mm. With OTS as antisticking layer, resist could be spincoated on top of the Si mold and all protrusions were filled. Of all three studied imprint techniques, only dlNIL has the ability to compensate for imperfectly filled mold protrusions in the imprinting process by resist flowing in from the substrate-deposited resist. This is especially beneficial for very large features and wavy surfaces, for instance foils.

Another unique benefit of dlNIL is the ability to pattern features on wavy foils by combining two resists with different etch properties. With a high enough etch selectivity toward RIE process gases, the inhomogeneous residual layer thickness given in the valleys and hills of the foil can be homogeneously removed without imprint pattern destruction.

A strong benefit from the dlNIL patterning technique is the smart combination of two resist with different properties. This allows extension to many resist combinations for tailored nanostructure fabrication. In this way, dlNIL will enhance the materials versatility of NIL, and contribute to the florishing field of nano- and microstructuring of functional materials, for example in combination with self-assembly.[26−29]

EXPERIMENTAL SECTION

Materials and Methods. 1H,1H,2H,2H-perfluorodecyltrichlorosilane (PFDTS, purity 97%) was purchased from ABCR GmbH & Co. KG. Octadecyltrichlorosilane (OTS, 95% purity) was purchased from Acros Organics. Thermoplastic resists mrI7020E and mrI-T85 were purchased from Micro resist technology GmbH. Poly(methyl methacrylate) (PMMA) was purchased from Aldrich and dissolved in Anisole. Teonex Q65a Polyethylene naphthalate foil (PEN, 125 μm thick) was purchased from Dupont Teijin. All materials were used as received without further purification.

Preparation of fluorinated molds. PFDTS was deposited overnight in a desiccator by chemical vapor deposition onto piranha cleaned Si-templates. The subsequent annealing step for 30 min at 100 °C was followed by 10 min ultrasonication in acetone. OTS was applied overnight from a 0.1 mM toluene solution and rinsing with toluene the day after.

Resist deposition. Thermoplastic resist mrI7020E (Microresist Technology GmbH, Berlin) was in all processes spincoated for 5 s at 500 rpm and 20 s at 3000 rpm on the substrate (Si and FOC), followed by a short baking step of 2 min at 120 °C on a hot plate for solvent evaporation. On the Si mold resist is deposited by spincoating 5 s at 500 rpm, 10 s at 1500 rpm, and 15 s at 3000 rpm resulting in a homogeneous layer and fully filled mold. A short baking step of 2 min at 120 °C on a hot plate was performed for solvent evaporation

Thermal imprinting. Thermal imprinting was performed with the Eitre 6 from Obducat (Malmö, Sweden). The best imprint results were obtained at an imprint temperature of 140 °C under 40 bar pressure for an imprint time of 300 s. Demolding occurred 5 °C below T_g, at 55 °C.

Residual layer removal. The thin residual layer left after imprinting is removed by anisotropic O_2 plasma based reactive ion etching. At a chamber pressure of 10 mTorr and 20 sccm O_2 the residual layer was removed within 2 min at 20 W.

Direct etching. The with RIE opened windows in the resist layer uncover the Au/Ti metal layer, which is removed by wet etching the 30 nm Au by 10 s exposure to a solution of KI:I_2:H_2O 4:1:40 and 15 s exposure of the 5 nm Ti adhesion layer to a 1% HF solution. After being thoroughly rinsed with Milli-Q water and N_2 blow drying, resist is stripped off by O_2 plasma treatment or by sonication in acetone.

Lift-off. After the residual layer was removed, 5 nm Ti and 30 nm Au were evaporated over the entire substrate. Resist and metal deposited on to the resist were removed by lifting of the resist in acetone, thoroughly rinsing with Milli-Q water and N_2 blow drying.

ASSOCIATED CONTENT

Supporting Information. Filling issues and dewetting results obtained for regular and reverse NIL with PFDTS as antisticking layer are given. This material is available free of charge via the Internet at http://pubs.acs.org.

AUTHOR INFORMATION

Corresponding Author
*E-mail: J.Huskens@utwente.nl.

ACKNOWLEDGMENT

The program Lithography on flexible substrates of the Holst Centre is acknowledged for financial support. Mark Smithers is thanked for the SEM images.

REFERENCES

(1) Schift, H. *J. Vac. Sci. Technol. B* **2008**, *26*, 458–480.
(2) Guo, L. J. *J. Phys. D: Appl. Phys* **2004**, *37*, R123.
(3) Chou, S. Y.; Krauss, P. R.; Renstrom, P. J. *Appl. Phys. Lett.* **1995**, *67*, 3114–3116.
(4) Chou, S. Y.; Krauss, P. R.; Renstrom, P. J. *Science* **1996**, *272*, 85–87.
(5) Tan, H.; Gilbertson, A.; Chou, S. Y. *J. Vac. Sci. Technol. B* **1998**, *16*, 3926–3928.
(6) Haatainen, T.; Ahopelto, J. *Phys. Scr.* **2003**, *67*, 357.
(7) Haatainen, T.; Mäkelä, T.; Ahopelto, J.; Kawaguchi, Y. *Microelectron. Eng.* **2009**, *86*, 2293–2296.
(8) Ruchhoeft, P.; Colburn, M.; Choi, B.; Nounu, H.; Johnson, S.; Bailey, T.; Damle, S.; Stewart, M.; Ekerdt, J.; Sreenivasan, S. V.; Wolfe, J. C.; Willson, C. G. *J. Vac. Sci. Technol. B* **1999**, *17*, 2965–2969.
(9) Colburn, M.; Grot, A.; Choi, B. J.; Amistoso, M.; Bailey, T.; Sreenivasan, S. V.; Ekerdt, J. G.; Willson, C. G. *J. Vac. Sci. Technol. B* **2001**, *19*, 2162–2172.
(10) Ahn, S. H.; Guo, L. J. *ACS Nano* **2009**, *3*, 2304–2310.

(11) Choi, S. J.; Yoo, P. J.; Baek, S. J.; Kim, T. W.; Lee, H. H. *J. Am. Chem. Soc.* **2004**, *126*, 7744–7745.
(12) Huang, X. D.; Bao, L.-R.; Cheng, X.; Guo, L. J.; Pang, S. W.; Yee, A. F. *J. Vac. Sci. Technol. B* **2002**, *20*, 2872–2876.
(13) Bao, L.-R.; Cheng, X.; Huang, X. D.; Guo, L. J.; Pang, S. W.; Yee, A. F. *J. Vac. Sci. Technol. B* **2002**, *20*, 2881–2886.
(14) Cheng, X.; Jay Guo, L. *Microelectron. Eng.* **2004**, *71*, 288–293.
(15) Rowland, H. D.; King, W. P. *J. Micromech. Microeng.* **2004**, *14*, 1625–1632.
(16) Hirai, Y.; Konishi, T.; Yoshikawa, T.; Yoshida, S. *J. Vac. Sci. Technol. B* **2004**, *22*, 3288–3293.
(17) Rowland, H. D.; Sun, A. C.; Schunk, P. R.; King, W. P. *J. Micromech. Microeng.* **2005**, *15*, 2414–2425.
(18) Scheer, H. C.; Bogdanski, N.; Shibata, M.; Möllenbeck, S. *Microelectron. Eng.* **2009**, *86*, 688–690.
(19) Kim, S. M.; Kang, J. H.; Lee, W. I. *Polym. Eng. Sci.* **2011**, *51*, 209–217.
(20) Kang, J.-H.; Kim, K.-S.; Kim, K.-W. *Appl. Surf. Sci.* **2010**, *257*, 1562–1572.
(21) Marín, J.; Rasmussen, H.; Hassager, O. *Nanoscale Res. Lett.* **2010**, *5*, 274–278.
(22) Schift, H.; Kim, G.; Lee, J.; Gobrecht, J. *Nanotechnology* **2009**, *20*, 355301.
(23) Rowland, H. D.; King, W. P.; Sun, A. C.; Schunk, P. R. *J. Vac. Sci. Technol. B* **2005**, *23*, 2958–2962.
(24) Borzenko, T.; Tormen, M.; Schmidt, G.; Molenkamp, L. W.; Janssen, H. *Appl. Phys. Lett.* **2001**, *79*, 2246–2248.
(25) Janssen, D.; De Palma, R.; Verlaak, S.; Heremans, P.; Dehaen, W. *Thin Solid Films* **2006**, *515*, 1433–1438.
(26) Escalante, M.; Zhao, Y.; Ludden, M. J. W.; Vermeij, R.; Olsen, J. D.; Berenschot, E.; Hunter, C. N.; Huskens, J.; Subramaniam, V.; Otto, C. *J. Am. Chem. Soc.* **2008**, *130*, 8892–8893.
(27) Escalante, M.; Lenferink, A.; Zhao, Y.; Tas, N.; Huskens, J.; Hunter, C. N.; Subramaniam, V.; Otto, C. *Nano Lett.* **2010**, *10*, 1450–1457.
(28) Duan, X.; Park, M.-H.; Zhao, Y.; Berenschot, E.; Wang, Z.; Reinhoudt, D. N.; Rotello, V. M.; Huskens, J. *ACS Nano* **2010**, *4*, 7660–7666.
(29) Duan, X.; Zhao, Y.; Berenschot, E.; Tas, N. R.; Reinhoudt, D. N.; Huskens, J. *Adv. Funct. Mater.* **2010**, *20*, 2519–2526.